# GenEpi: Gene-based Epistasis Discovery Using Machine Learning

Yu-Chuan Chang[1], June-Tai Wu[2], Ming-Yi Hong[3], Yi-An Tung[4], Ping-Han Hsieh[1], Sook Wah Yee[5], Kathleen M. Giacomini[5,6], Yen-Jen Oyang[1], and Chien-Yu Chen[3,*], for the Alzheimer's Disease Neuroimaging Initiative†

[1]Graduate Institute of Biomedical Electronics and Bioinformatics, National Taiwan University, Taipei 10617, Taiwan. [2]Department of Dermatology, National Taiwan University Hospital, Taipei 10002, Taiwan. [3]Department of Bio-Industrial Mechatronics Engineering, National Taiwan University, Taipei 10617, Taiwan. [4]Genome and Systems biology degree program, Academia Sinica and National Taiwan University, Taipei 10617, Taiwan. [5]Department of Bioengineering and Therapeutic Sciences, University of California, San Francisco, San Francisco, California, USA. [6]Institute for Human Genetics, University of California, San Francisco, San Francisco, California, USA.

*To whom correspondence should be addressed.

†Data used in preparation of this article were obtained from the Alzheimer's Disease Neuroimaging Initiative (ADNI) database (adni.loni.ucla.edu). As such, the investigators within the ADNI contributed to the design and implementation of ADNI and/or provided data but did not participate in analysis or writing of this report. A complete listing of ADNI investigators can be found at:
https://adni.loni.usc.edu/wp-content/uploads/how_to_apply/ADNI_Acknowledgement_List.pdf

Chien-Yu Chen
Department of Bio-Industrial Mechatronics Engineering, National Taiwan University, Taipei 10617, Taiwan.
Phone: +886-2-3366-5334, E-mail: chienyuchen@ntu.edu.tw

## Abstract

**Motivation:** Genome-wide association (GWA) studies provide a powerful means to identify associations between genetic variants and phenotypes. However, GWA techniques for detecting epistasis, the interactions between genetic variants associated with phenotypes, are still limited. We believe that developing an efficient and effective GWA method to detect epistasis will be a key for discovering sophisticated pathogenesis, which is especially important for complex diseases such as Alzheimer's disease (AD). In this regard, this study presents GenEpi, a computational package to uncover epistasis associated with phenotypes by the proposed machine learning approach, and illustrates the application of GenEpi on predicting the diagnosis and the progression of AD.

**Methods:** The key concept of GenEpi is a feature extraction process based on gene structures. Since a gene is the minimal physical and functional unit of heredity, GenEpi considers a gene as a unit to retrieve genetic variants as features. GenEpi adopts two-element combinatorial encoding when producing features and constructs the prediction models by randomized regression. Features are first modeled using combinatorial encoding followed by randomized regression to detect the epistasis within a single gene. The selected features for each gene are then pooled together to identify cross-gene epistasis, using randomized regression again. This

study uses AD as an example to reveal the capability of GenEpi in finding disease-related variants and variant interactions that show both biological meanings and predictive power.

**Results:** This study compared GenEpi with several commonly used algorithms for detecting epistasis, including FastEpistasis, BOOST and ReliefF. The simulation data demonstrated that GenEpi outperforms the other methods in ranking the true epistasis as the top one. As real data is concerned, the results suggest that the epistasis selected by GenEpi has the best predictive power for two major phenotypes in the AD dataset: diagnosis of AD and disease progression. For diagnosis, the proposed model of predicting AD contains three clinical features (Age, Gender and Education) and 14 genetic features, including 24 SNPs from 12 genes that contain the well-known causal gene, APOE. The 2-fold cross validation (CV) and leave-one-out CV (LOO CV) accuracy of this model are 0.83 and 0.81, respectively. On the other hand, for predicting progression, the proposed model contains eight clinical features (Age, Gender, Education, Cognitively Normal (CN), Early Mild Cognitive Impairment (MCI), Late MCI, AD, and MMSE at baseline) and four genetic features, including seven SNPs from six genes, where all of the four genetic features are cross-gene epistasis with significant p-values ($< 10^{-11}$). The average of Pearson and Spearman correlation of 2-fold CV and LOO CV are 0.52 and 0.53, respectively. The results on AD demonstrated that GenEpi has the ability to detect the epistasis

associated with phenotypes effectively and efficiently. The released package can be generalized to largely facilitate the studies of many complex diseases in the near future.

**Availability:** GenEpi is an open-source python package and available free of charge only for non-commercial users. The package can be downloaded from https://github.com/Chester75321/GenEpi, and has also been published on The Python Package Index.

## Introduction

Genome-wide association studies (GWAS) is a univariate examination of a genome-wide set of genetic variants to determine if any single variant is associated with the phenotype of interest [1]. The first GWAS was published in 2002 [2], and three years later, the most remarkable GWAS regarding age-related macular degeneration (AMD) was published [3]. Their study investigated the association of 105,980 single nucleotide polymorphisms (SNPs) with AMD on 96 cases and 50 control subjects. This study showed that the SNPs in the complement factor H (CFH) gene, including a non-synonymous SNP, are significantly associated with AMD. Up to 2017, there have been more than hundreds of thousands individuals being studied in typical GWAS protocols, and over 72,870 variant-disease associations between 46,589 SNPs and 6,356

phenotypes have been discovered [4]. These studies demonstrated the potential of GWAS to identify genetic variants associated with many categories of phenotypes, including risk for diseases such as various cancers, and variation in therapeutic and adverse response to drugs. However, the success of univariate GWAS is limited to monogenic phenotypes (e.g. Mendelian diseases). The impact of variant interactions, also known as epistasis on the formation of diseases [5] is often underestimated in traditional GWAS analysis [6-8].

Researchers have found that GWAS has limitation in identifying the association in complex diseases [9, 10]. Easton et al. suggested that a number of susceptible loci identified by GWAS usually have very small effect sizes [11]. A major disadvantage of GWAS is that it considers only one genetic variant at a time, and ignores underlying epistasis of variants that might have stronger associations [12]. Studies have also demonstrated that the existence of epistasis is an important factor contributing to phenotypes, especially in complex diseases such as hypertension, diabetes and obesity [10]. Therefore, developing analytical methods to identify epistasis efficiently is critical to understanding the genetic factors that contribute to human traits [8, 13], and has attracted a wide range of research interests in recent years [7, 14].

Two main challenges to discover epistasis are computational complexity and statistical power [15]. The first challenge results from the curse of dimensionality. When more genetic variants

are considered, the number of interactions increases exponentially. Based on the specification of a major commercial technology, Illumina Arrays, a whole-genome array can investigate over 4 million markers per sample simultaneously. In order to evaluate the pairwise interactions from this microarray, about $8\times10^{12}$ statistical tests need to be processed. Even though Marchini et al. have demonstrated that pairwise interactions of $3\times10^{5}$ loci is computationally possible with currently available computational resources, it still remains challenging when the Illumina Arrays are considered [16]. The second challenge is the issue of statistical power. Since a huge number of statistical tests are conducted on a limited sample size with high-dimensional interactions, many false positives arise by random chances. In this regard, new methods have been developed [10, 17]. Statistical approaches include FastEpistasis [18] and BOOST [19]; the later one has been included in a well-known GWAS software called PLINK [20, 21]. Machine learning approaches such as Multifactor Dimensionality Reduction [22], ReliefF [23], random forest-like algorithms [24-26] and other methodologies have also been developed for detecting epistasis [17].

Since the biological experiments used to validate these methodologies are still in demand, there are no standard analysis methods for epistasis despite the rapid improvement in computational performance. In 2016, Murk used FastEpistasis and BOOST to search SNP-SNP interactions

on a huge dataset called Genetic Epidemiology Research on Adult Health and Aging (GERA) that included 78,486 subjects, but still failed to detect a significant and replicable interaction after exhaustively searching through 45 billion possible interactions for 10 complex diseases of interest [27]. Alzheimer's disease (AD) is one of these complex diseases and its pathogenesis, which clearly has a genetic basis, is still ill-defined. In 2016, Sage Bionetworks held a competition called The Dialogue for Reverse Engineering Assessments and Methods Challenge (DREAM Challenge) for AD, which tried to use crowdsourcing to assess the capability of current computational methods to predict the change in cognitive examination based on genetic data. However, no significant contribution of genetic features except the *APOE* haplotype to the predictive performance was observed by any competition teams [28]. To address this problem, this study presents GenEpi, a package to reveal epistasis related to the phenotype using machine learning and introduces the application of GenEpi on predicting the diagnosis and the progression of AD.

## Methods

The architecture of GenEpi is shown in Fig. 1. GenEpi is designed to group SNPs by gene boundaries. GenEpi first considers the genetic variants in a gene as features, which have a

higher chance to interact with each other and to influence molecular functions. The idea of within-gene epistasis analysis followed by cross-gene analysis is not new, which has also been used in previous studies [29-32]. Differently, GenEpi adopts two-element combinatorial encoding when producing features and models them by randomized regression, which will be explained in Section 2.2. In the first stage (STAGE 1) of GenEpi, the genotype features from each single gene will be combinatorically encoded and modeled independently by randomized regression. In this way, we can estimate the prediction performance of each gene and detect within-gene epistasis with a low false positive rate. In the second stage (STAGE 2), both of the individual SNP and the within-gene epistasis features selected by STAGE 1 are pooled together to generate cross-gene epistasis features. Finally, the genotype features after feature selection are combined with environmental factors such as clinical features to build the final prediction models. In addition to the main procedures, two pre-processing steps are also implemented in GenEpi: retrieving the gene information from public databases and reducing the gene information from public databases and reducing the dimensionality of the features using linkage disequilibrium (LD). In the end, we released a Python package that implements GenEpi (main steps are illustrated in Supplementary Fig. S1). The details of these steps and the GenEpi method will be described in the following sections.

**University of California Santa Cruz (UCSC) database**

To obtain the gene information such as official gene symbols and genomic coordinates, we retrieved kgXref and knownGene data table from the UCSC human genome annotation database [33, 34]. The version of the database we used is the Feb. 2009 assembly of the human genome hg19, GRCh37 Genome Reference Consortium Human Reference 37. The two data tables were merged in order to generate a local database containing the gene symbols as well as the genomic coordinates of each gene. The in-house script we built could update this local database automatically. It is noted that there are many different categories of genes in the RefSeq database. In this study, we only focused on the mRNA and non-coding RNA (22,376 genes in total). The selected transcripts were projected on the genomic coordinates and the coordinates of corresponding genes were determined based on the leftmost and rightmost positions of the corresponding transcripts. Moreover, to discover the factors that might affect the transcription of genes, we also retained the promoter region of each gene. In genetics, the promoter region is a segment of DNA that initiates the transcription of a particular gene. Promoters are located near the transcription start sites of genes, on the upstream of the same DNA strand (towards the 5' region of the sense strand of the transcript). In general, a promoter

region can be 100-1000 base pairs long. In this study, we extracted 1,000 nucleotides on the upstream of the starting position of each gene as the promoter region.

**Estimation of linkage disequilibrium**

In GWAS datasets, a SNP often exhibits high dependency with its nearby SNPs because of linkage disequilibrium (LD). In the practical implantation, we prefer to group these dependent features to reduce the dimension of features. In other words, we can take the advantages of LD to reduce the dimensionality of SNP features. In this regard, we adopted the same approach developed by Lewontin [35] to estimate LD. We used $D'>0.9$ and $r^2>0.9$ as the criteria to group highly dependent SNP features as blocks. In each block, we chose the features with the largest minor allele frequency to represent other features in the same block.

**Discovery of within-gene epistasis**

The main objective of the first stage in GenEpi is to select candidate features from each gene. In order to extract SNP features for a gene, we used the start and end positions of each gene from the local UCSC database to split the SNP features after dimension reduction. Since there are 22,376 genes in the UCSC database, we obtained 22,376 subsets of the SNP features. In

each subset, A SNP feature with the alleles 'A' and 'a' could have three possible genotypes, AA, Aa and aa, which are used to refer to the pairs of alleles. The pairs of alleles are subsequently separated into three binary features using one-hot encoding. In order to evaluate epistasis, we generated interacting features by crossing each pair of genotype features. Considering the false positive rate and computational complexity, we only focused on pairwise interactions of epistasis throughout this study. We defined the interaction between two SNPs in following equation, $\boldsymbol{\alpha_1 SNP_1} + \boldsymbol{\alpha_2 SNP_2}$ stand for the additive interactions and $\boldsymbol{\alpha_{int(1,2)} SNP_1 \otimes SNP_2}$ represents the synergistic interactions that contain nine terms shown in equation.

$$y \sim \alpha_0 + \sum_{m \in \{AA,Aa,aa\}} \alpha_{1,m} SNP_{1,m} + \sum_{m \in \{AA,Aa,aa\}} \alpha_{2,m} SNP_{2,m} + \sum_{m,n \in \{AA,Aa,aa\}} \alpha_{1,m,2,n} SNP_{1,m} SNP_{2,n}$$

$$= \alpha_0 + \alpha_1 SNP_1 + \alpha_2 SNP_2 + \alpha_{int(1,2)} SNP_1 \otimes SNP_2$$

Before modeling each subset of genotype features, two criteria were adopted to exclude low quality data. The first criterion is that the genotype frequency of a feature should exceed 5%, where the genotype frequency means the proportion of genotype among the total samples in the dataset. The second criterion is regarding the association between the feature and the phenotype. If the phenotype is dichotomous or categorical, the p-value of $\chi^2$ test should be smaller than 0.01. If the phenotype is a real number, we used F-test to estimate the correlation between the feature and the phenotype, and the p-value should be smaller than 0.01. In the end, a gene may

have multiple SNPs. The general form of the linear model for a gene with $k$ SNPs is defined as following equation, which be termed two-element combinatorial encoding.

$$y \sim \alpha_0 + \sum_{i=1}^{k} \alpha_i SNP_i + \sum_{i=1}^{k} \sum_{j=1 \cap j \neq i}^{k} \alpha_{int(i,j)} SNP_i \otimes SNP_j$$

We conducted Randomized Lasso and L1-penalized Logistic regression for modeling each gene. The first advantage is that the L1-penalized model prefers solutions with a smaller number of features, which effectively reduces the effect of feature dependency. The second advantage is by using randomization techniques [36], we can largely reduce the false positive rate. Randomized regression works by resampling and remodeling the training set hundreds or thousands of times, followed by picking out the features that are repeatedly selected across randomization. In this study, we executed this randomization 500 times, and the features selected by randomization would be retained for the next stage.

**Discovery of cross-gene epistasis**

In the second stage, we used the features selected by STAGE 1 to generate cross-gene epistasis features and then applied the same selection procedure described in Section 2.3 to find the cross-gene epistasis that are associated with the phenotype. The procedures were slightly modified here. Since we only focused on pairwise interactions, instead of using the entire

features we selected in STAGE 1, we only used single-SNP features to generate cross-gene epistasis features. Also, we used the genotype frequency and the p-values of $\chi^2$ test or F-test to control the quality of features and to avoid overfitting. Nevertheless, the p-value of each feature in this stage should be smaller than $10^{-5}$. All of the features from different genes would be merged for modeling cross-gene epistasis. We conducted Lasso and L1-penalized Logistic regression for modeling, and the randomization techniques were used once again to select the final genotype feature set. Since the phenotype may also be affected by environmental factors, after determining the final set of genotype features, we included the environmental factors such as clinical assessments for constructing the final model. To obtain the final model, we used random forests with 1,000 decision trees as the ensemble algorithm. Subsequently, the final model was evaluated through a process called double cross validation (CV). In the external loop of double CV, all the instances were divided into two subsets to serve as training and independent test sets. In this study, we used 2-fold CV and leave-one-out CV (LOO CV) in external loop for evaluation. In the internal loop, we also used 2-fold CV for model selection.

## Materials

This study applied GenEpi on an AD cohort, which was used in Alzheimer's disease Dream

Challenge [28], In total, the cohort consists of 767 participants, who were healthy elderly, mild cognitive impairment (MCI) and AD patients from the Alzheimer's Disease Neuroimaging Initiative (ADNI) database. The 767 ADNI participants consist of 241 cognitively normal (CN), 130 Early MCI (EMCI), 273 Late MCI (LMCI) and 123 AD participants. We adopted two types of features in this study: clinical and genetic data. The clinical assessment includes the 'Mini-Mental State Examination (MMSE) at baseline' and the '24-month follow-up MMSE'. Other clinical measures included 'diagnosis at baseline', 'age at baseline' (Age), 'years of education at baseline' (Education), 'gender' (Gender), and '*APOE* genotype'. All the genetic data has been pre-processed by the organizers that held the challenge [28]. The genetic data were genotyped using the Illumina Human610-Quad BeadChip and Illumina HumanOmniExpress BeadChip. The multidimensional scaling analysis was applied by PLINK using HAPMAP3 to ensure that samples are within the cluster of European populations. Subsequently, the data were imputed according to the 1,000 genome haplotypes. After imputation, there were 12,809,667 genotype features in total. Because GenEpi can be applied to solve both classification and regression problems, this study illustrated both applications of GenEpi on the ADNI cohort. In predicting the diagnosis of AD, we used 364 participants, of which the clinical diagnosis are CN or AD, to predict which samples are control subjects or the AD patients. For predicting the progression

of AD, we used the MMSE difference between '24-month follow-up MMSE' and 'MMSE at baseline' as the predicting targets.

## Experimental Results

This section includes four parts. In the first part, we applied GenEpi and other algorithms for detecting epistasis, including FastEpistasis [18], BOOST [19] and ReliefF [23, 37] on simulation data for validation and comparison. In the second part, we applied GenEpi on the ADNI dataset to categorize each sample as control subjects or AD patients, evaluated by precision, recall, accuracy and F1 score (2 × (precision × recall) / (precision + recall)). In the third part, we used the same dataset to predict the progression of AD, which is being defined as the MMSE difference between the baseline and the follow-up after 24 months, and the performance was assessed using Pearson correlation and Spearman correlation between the predicting results and the MMSE differences. In the final part, we compared GenEpi with other algorithms on the ADNI dataset in terms of computing time and prediction performance on real data.

### Experiments on simulation data

In this section, we applied different algorithms on simulation data for validation and comparison. All of the simulation datasets are generated by the simulator GAMETES [38], which is publicly accessible on the web site https://popmodels.cancercontrol.cancer.gov/gsr/packages/gametes/. We designed two types of simulation datasets: basic and complex models. The 'Model 1', 'Model 2' and 'Model 3' are simulation datasets with the basic model, which means that each dataset contained only one epistasis consisting of a SNP pair. All of the basic-model datasets are in the same setting as follows: #individuals = 2000, case/control ratio = 1, #SNPs = 100, #replicates = 100, minor allele frequency of target SNPs = 0.2, and heritability = 0.2. The complex model means one dataset contains multiple epistasis from different SNP pairs. Here, the 'Combined Model 1+2+3' is a complex model dataset containing three epistasis from the previous three basic models.

Fig. 2 provided the results of these four simulation datasets. Fig. 2(a) shows that the ranking of the target epistasis reported by GenEpi in the 100 replicates of each basic-model dataset are always ranked as the first. In contrast, for FastEpistasis and BOOST, the medians of the ranking of the target epistasis among the 100 runs of simulation are one but the averages are not. The number of failures of FastEpistasis and BOOST in 100 replicates of three basic models are 6, 1, 16 and 5, 1, 14, respectively, which means that the ranked lists contain some false positive

epistasis when the ground truth is single target epistasis. For the result of the complex model dataset in Fig. 2(b), the superiority of GenEpi over other algorithms is more obvious. In the 100 runs of simulation, GenEpi reported the three target epistasis as the top three important features every time. In contrast, FastEpistasis and Boost failed to report the three target epistasis as the top three important features consistently.

When ReliefF was compared, since the Python package scikit-rebate [37] that we used for implementing ReliefF only reports the importance of individual SNPs instead of the scores for epistasis (SNP pairs), we listed the medians of ReliefF's ranking for each SNP in the pair in Table 1. Table 1 reveals that ReliefF can detect the SNPs in the target epistasis in the basic models, but produced some false positives in the complex model dataset.

We considered that the superiority of GenEpi is owing to the proposed two-element combinatorial encoding of the genotype features and the randomization technique. In contrast with other statistical algorithms such as FastEpisasis and BOOST, which only evaluate the epistasis of a SNP pair one at a time, GenEpi considers interactions between combinatorial features by multivariate models. Moreover, the false positives among the epistasis can be filtered out by resampling and remodeling the dataset hundreds or thousands of times. To evaluate the effect of randomization, we applied both randomized regression and original

regression on the complex model dataset to compare the number of false positives, which is defined as the number of non-target epistasis in the final output of GenEpi. As shown in Fig. 3. randomized regression can reduce the mean false positive rate effectively and minimized the variance of false positive rate as well. For other methods, this information is not available because they output all the pairs of SNPs as a ranking list.

**Classification – Classifying AD patients**

In predicting control subjects or AD patients, we applied GenEpi on the 364 samples with CN (as control) or AD. After dimensionality reduction, 12,102,888 out of the 12,809,667 SNPs in the ADNI dataset were retained, and 4,916,249 of them are located in 20,206 genes (Table 2). In the step 4 of selecting epistasis, there are 34,689 genetic features selected and 765 of them are single SNP features, while the other 33,924 are epistasis features within genes. The final model contained 3 clinical features (Age, Gender, and Education) and 14 genetic features, including 24 SNPs from 12 genes. These features contained two single SNP features, 11 within-gene epistasis features and one cross-gene epistasis feature.

To validate the effectiveness of the genetic features extracted by GenEpi, we compared different subsets of the features in Table 3. The performance of the model considered only clinical

features outperform that considered only genetic features. When we combined both kind of features, the performance improved, showing that added genetic features is effective. To reduce the redundancy, we removed '*APOE* genotype', which can be replaced by the genetic features selected by GenEpi. We also removed 'MMSE at baseline', which is a clinical assessment to measure the cognitive impairment. We argued that it does not make sense to use 'MMSE at baseline' as a feature to predict the status of AD at the moment of diagnosis. The last two columns of Table 3 showed that the model that used both genetic and clinical features without *APOE* genotype and 'MMSE at baseline' is significantly better than the one that considered only clinical features.

We listed the statistical significance of the selected genetic features in Table 4. The first column lists each feature by its RSID (Rapid Stain Identification Series) and the genotype (denoted as RSID_genotype), the pairwise epistasis features are represented using two SNPs. The last column describes the genes where the SNPs are located according to the genomic coordinates. We used a star sign to denote the epistasis between genes. Here, only the feature (rs3130614_BB, rs41276317_AB) is cross-gene epistasis (for MICB and TOB2). The weights in the second column were extracted from the linear model we defined in Section 2.4. The signs of the weights indicate if a feature is a causal or protective genotype. On the other hand, the

odds ratio significantly away from 1 also indicates whether the features are potential causal or protective genotypes. Since low genotype frequency may cause unreliable odds ratios, we also listed this information in the table. Lastly, the p-value of the $\chi^2$ test showed that these features are significantly associated with the phenotype. Figure 5 are the bar plots for the features selected by GenEpi shown in Table 4. We took one single-SNP and the cross-gene epistasis features as examples. Since each SNP pair has nine SNP combinations, we used the color 'light blue' to highlight the features selected by GebEpi. We considerd that a good feature can be judged by two conditions. The first one is that the difference between the amount of case and control subjects should be large, which suggests that the case and control subjects can be distinguished by this feature. The second one is that the genotype frequency of this feature cannot be too small, which suggests that the occurrences of this feature are not only supported by a small number of samples. Fig. 5(a) reveals that rs429358_AA is a good feature, because the number of samples in the light blue cell is about 60 percent of the whole dataset and the proportion of control versus case is 4.425:1. This feature is actually a single SNP feature located on *APOE*. Moreover, it is a well-known SNP for determining the allele type of *APOE*. Fig. 5(b) showed all combinations of the SNPs rs3130614 and rs41276317. Even though the number of samples in the light blue cell is not particularly large, it can still be considered as a good feature

with following explanation. By examining the cells in this figure, two of them are empty cells, one of them has only one sample, and another five cells have more control subjects than cases in the cells. Since the proportion of control subjects and cases of this dataset is 2:1, the samples seem to be randomly distributed into these five cells. In contrast, the proportion of the control subjects and cases is 1:8 in the light blue cell in the opposite, which indicates the SNP pair with such combination can be considered as a potential causal genetic variant for AD. These results show that GenEpi has the ability to identify good features.

**Regression – Predicting the progression of AD**

In predicting the progression of AD, we applied GenEpi on all of the samples from ADNI. For this task, the 'diagnosis at baseline' and 'MMSE at baseline' were also adopted as clinical features. After LD dimension reduction, the original 12,809,667 SNPs decreased to 12,507,343, and 5,086,639 of them are located on 20,206 genes (Table 2). After selecting epistasis by Step 4, there are 56,427 genetic features left, and 1302 of them are single SNP features, while the other 55,125 are epistasis features in a single gene. The proposed model contained eight clinical features (Age, Gender, Education, CN, EMCI, LMCI, AD, and MMSE at baseline) and four genetic features, which included seven SNPs from six genes, and all of the four genetic features

are cross-gene epistasis. We compared different subsets of features in Table 5. The performance of the model that only included genetic features is lower than the one that only included the clinical features. However, when we combined both of them, the performance improved, similar to the situation observed in the task of classification. It shows that the genetic features are effective. Again, the *APOE* genotype in the clinical feature set is a genetic feature in essence. So, we removed it from the list of clinical features. The last two columns showed that even though we removed the *APOE* genotype, the model with genetic features are still better than the model without the genetic features. The weights in Table 6 were extracted from the linear model we described in Section 2.4. The signs of the weights indicate whether the feature is a causal or protective gene. We applied student's t-test on the samples with the combination of the selected genetic features (Fig. 6), and all of the p-values of t-test are significant ($< 10^{-11}$). These results show that GenEpi has the ability to identify good features in the regression task, too.

**Comparison with different algorithms**

In this section, we compared GenEpi with other algorithms for detecting epistasis, including FastEpistasis [18], BOOST [19] and ReliefF [23] in terms of computing time and prediction

performance. We used Microsoft Azure E32 v3 as the computing resource, which contains 32 CPUs and 256 GB RAM. Since the second generation of PLINK has imported FastEpistasis and BOOST, we used PLINK to test these two algorithms. For ReliefF, we employed a Python package called scikit-rebate [37] for implementation. Among these algorithms, only FastEpistasis can afford the computation of the whole set of SNPs. In this regard, 12,809,667 SNPs were used by FastEpistasis (Table 7). However, since FastEpistasis only supports the classification trial in PLINK, it was skipped in the task of regression. On the other hand, GenEpi only focuses on the SNPs in the gene regions. In this regard, the number of input SNPs for estimating epistasis reduced to 4,916,249 and 5,086,639 in classification and regression tasks, respectively. BOOST took the same subsets of SNPs as GenEpi (Table 7). When taking the same subset of SNPs as GenEpi and BOOST, ReliefF still caused memory errors. Therefore, we used the subsets of SNPs that selected by STAGE 1 of GenEpi as the input of ReliefF, which are 33,868 and 69,842 in classification and regression tasks, respectively. We selected the top 15, 30, 45 and 60 rankings from the results of these algorithms for comparing the prediction performance. Since different algorithms adopted different strategies to estimate the importance of the feature, we adopted different formulas defined in Section 2 to generate features for prediction. FastEpistasis and BOOST used $\chi^2$ statistics to rank the SNP pairs. For these two

algorithms, we put the top SNP pairs into Equation 2 to generate pairwise interactions for each pair. ReliefF reported significance scores for each SNP, but we cannot find a way to know the relations between these SNPs. Therefore, we used Equation 3 to generate the interactions for all the combinations of SNP pairs. Finally, we used logistic and lasso regression to build the models for classifying AD patients and predicting the progression of AD for comparison. Table 7 show that GenEpi is the most efficient method, which only cost 9.95 and 28.38 CPU-days in classification and regression tasks, respectively. In both classification or regression tasks, GenEpi had the best prediction performance despite the fact that GenEpi only uses the subset of SNPs from the final model. GenEpi shows that the time needed for identifying epistasis can be drastically reduced, without compromise to the performance. We provided the ROC curves for the classification task in Fig. 7, and it shows that GenEpi achieved the best performance in both training and double 2-fold CV procedures, of which the area under the curve (AUC) are 0.95 and 0.85, respectively.

## Discussion

The results in the previous section revealed the power of GenEpi to identify phenotype-associated epistasis efficiently. GenEpi selected 14 features from 12 genes to categorize patients

with AD and four features from six genes to predict the progression of AD. Since AD is a chronic neurodegenerative disease, our findings would be supported if the gene identified by GenEpi are expressed in brains. We downloaded the datasets of the GTEx Project [39] to inspect the gene expression of these genes in different tissues, as shown in Figure. 6. Among the 18 genes selected by GenEpi, 13 have high expression level in the brain tissues. In addition, five genes, *VSNL1*, *PRKAG2-AS1*, *SYT6*, *CLEC1A* and *LINC00299*, have a similar expression pattern with *APOE*. These 18 genes are categorized as cross-gene epistasis, single-gene epistasis and single-SNP features based on the feature types selected by GenEpi. The detail discussion about these three types of feature will be describe in following sections.

**Cross-gene epistasis**

GenEpi picked out five cross-gene epistasis in total, which include *CLEC1A * GPR142, CLEC1A * PRKAG2-AS1, IFT20 * RPL32, MFSD6L * PRKAG2-AS1* and *MICB * TOB2*. We found several direct and indirect evidence to demonstrate that these interactions might have true association with AD. Liddelow et al. found that neurotoxic reactive astrocytes are induced by activated microglia [40] and thus are implicated in AD [41]. The expression of *CLEC1A*, a phagocytic receptor gene, increased in aged microglia, indicative of a pro-inflammatory status

[42]. Based on HaploReg [43], the enhancer of *GPR142* is DNAse sensitive in primary astrocytes. Together evidence suggests that *CLEC1A* and *GPR142* are expressed in two inflammatory cells strongly related in AD. Li et al. found that *PRKAG2-AS1* and *PRKAG2* were differentially regulated [44], suggesting a possible negative regulatory role of *PRKAG2-AS1* on the *PRKAG2* mRNA level. The *PRKAG2*, AMP-activated protein kinase subunit gamma-2, has a polymorphism associated with cognitive impairment as well as diabetes in old age [45]. AMPK activation is also related to cognitive impairment in old age, neuroinflammation, and neurodegeneration [46]. Together, the epistasis between *PRKAG2-AS1* and *CLEC1A* raises an interesting possibility that *PRKAG2-AS1* may functionally interact with *CLEC1A* through AMPK regulated neuroinflammation.

We did not find direct link between *RPL32* and AD, but by the data presented in HaploReg there is another gene called *IQSEC1* that is located in the same LD block with *RPL32*. *IQSEC1* is expressed in neuron and physically binds to *APOE*, but the implication of this interaction in AD is not clear. *IFT20* is an essential component of primary cilia that appears to be important in the survival of dentate granule cell, which plays a key role in memory formation and related to AD [47]. These studies showed that *IFT20* and *IQSEC1* have been independently implicated in AD and our results suggest they might together maintain an intact primary cilia that functions

critically in AD. MIC proteins are induced on the cell surface by stress and are ligands of a common activatory natural killer-cell receptor (*NKG2D*) [48]. They thus have roles in antimicrobial defense, tumor suppression and autoimmune-like diseases [49]. Quiroga et al. has found that the human MHC class I chain-related genes (*MICA* and *MICB*) are located within the HLA region that has stratified association with AD in the cohort of the Oxford Project to Investigate Memory and Ageing (OPTIMA) even though the association did not survive the correction for multiple testing [50]. *TOB2* has been reported as a most up-regulated gene [51] by expression analysis on multiple AD expression datasets from the GEO database to identify significant genes associated with electrophysiological pathways and attempted determination of interconnected canonical molecular pathways. The interaction of *MICB* and *TOB2* suggests a not-yet-explored biological process in AD pathogenesis. However, the significant associations of these genes in genome-wide association studies associated with immune system diseases and neurological diseases (see GWAS Catalog, 22561518, 29083406, 28540026), warrant future investigation. Among all the cross-gene epistasis selected by GenEpi, only one gene *MFSD6L* cannot find the association with AD so far.

**Single-gene epistasis**

There are several possible modes of action accounting for intramolecular SNP-SNP interactions identified in this study. First: a synergistic regulation of transcription. For example, rs12095538 resides in the eQTL of STY6 and rs2774308 resides in a DNAse region of STY6. It is very possible that variants in both rs12095538 and rs2774308 synergistically affect the expression of STY6. SYT6 encodes protein control neurotransmitter release. It has been shown that the expression of SYT6 is significantly down regulated in AD [52], supporting the causative role of the inherited rs12095538 and rs2774308 haplotype in AD progression. Likewise, rs56233035 and rs3678 reside in the LD blocks containing the eQTL and DNAse region of CACNA1E, respectively. CACNA1E encodes a subunit of CaV1.2 calcium channel. Its expression level in reactive astrocytes is associated with amyloid-β plaques formation in an AD mouse model [53]. Another examples are the interactions between rs12926153 and rs12922908, and rs9652600 and rs12922908 that are within DNAse regions controlling the expression of CLEC16A in brain. CLEC16A encodes a lectin receptor involved in inflammation process and is differentially expressed in AD brains [54]. Lastly, rs2052573 and rs34580133 reside in DNAse regions within the LINC00299 and thus may synergistically control the expression of this long non-coding RNA that has been implicated in brain development [55].

Second: a synergestic interaction between transcriptional and post-transcriptional regulation.

For example, rs9344977, in an intron of BACH2 containing cis-regulatory elements, may affect the expression of BACH2, whereas rs56148686 in another intron of BACH2 without any cis-regulatory element. We suspect that rs56148686 may interact with s9344977 through a post-transcriptional mechanism such as RNA stability, RNA splicing, or microRNA binding. BACH2 encodes a transcription factor involving cellular responses toward oxidative stress. Interestingly, BACH2 is upregulated in cultured human neuroblastoma cells upon exposure to Alzheimer Amyloid β [56]. Similar mechanisms may apply to interaction pairs rs12189429-rs6881360 and rs12187423-rs6881360 that presumably regulating the abundance of ADAMTS12 mRNA. The importance of ADAMTS12 in AD is supported by another independent study using same ANDI dataset [57]. Third: an intramolecular SNP pairs modulating the expression of two separate neighboring genes. For example, rs11675339 and rs2710687 of VSNL1 appear to control the expression of GEN1 and SMC6 respectively. We also found that VSNL (also known as VILIP-1) has strong evidences to AD [58-60]. GEN1 and SMC6 play pivotal roles in repairing double-strand breaks of genomic DNA. Interestingly, rDNA instability, a result of failures to repair double-strand breaks of genomic DNA, has been implicated in AD [61]. Most of the single-gene epistasis selected by GenEpi can be explained by these three possible modes and only two of the significance SNP-SNP interactions are not

immediately clear at this moment. For example, rs12366151 resides in the eQTL of MICALCL, an AD associated gene [62] but the interacting rs10831829 resides in the intron of PARVA, a gene not-yet-reported to be associated with AD. Similarly, rs2421701 and rs200512701 reside in two eQTLs regulating TNKS2 expression. However, the ADP-ribose polymerase functionally contributes to AD is not clear.

**Single-gene epistasis**

There are only two single-SNP features and both of them are located in *APOE*, which is a well-known causal gene of AD, revealing that GenEpi is an effective tool to identify disease-causing genes. Moreover, GenEpi successfully selected out the SNP rs429358, which determines the allele type of *APOE* with rs7412.

## Conclusion

While GenEpi has shown its ability to identify epistasis efficiently, it might still has the following limitations. Firstly, GenEpi can only detect pairwise interactions. Second, GenEpi is a memory-consuming package, which might cause memory errors when calculating the epistasis of a gene containing a large number of SNPs. We recommend that the memory for

running GenEpi should be over 256 GB. Finally, a small sample size may lead overfitting, which forces us to use strict thresholds during feature selection. In this way, GenEpi delivers a high precision rate, but might suffer having false negatives. This implies different GWAS data might detect different sets of true positives. In summary, the results of this study demonstrated that GenEpi is a promising software package to identify causal SNPs and epistasis in GWAS, and it can be further used to predict the phenotypes. With the demonstrated efficiency, GenEpi is a powerful tool to explore gene-gene interactions that underlie complex diseases.

# Tables

**Table 1.** The medians of the rank of the target epistasis for ReliefF

| | SNP 1 | SNP 2 | SNP 3 | SNP 4 | SNP 5 | SNP 6 |
|---|---|---|---|---|---|---|
| Basic-model | 1 | 2 | 1 | 2 | 1 | 2 |
| Complex-model | 7 | 8.5 | 9.5 | 11.5 | 11 | 19.5 |

**Table 2.** The summary of the number of features after feature selection in the classification and regression tasks, respectively.

| Step | Classification | Regression | Unit |
|---|---|---|---|
| 0 (raw data) | 12,809,667 | 12,809,667 | SNP |
| 1 | 22,376 | 22,376 | Gene |
| 2 | 12,102,888 | 12,507,343 | SNP |
| 3 | 4,916,249 | 5,086,639 | SNP |
| | 20,206 | 20,206 | Gene |
| 4 | 44,865 | 69.843 | SNP |
| | 7,933 | 9,561 | Gene |
| | 34,689 | 56,427 | Feature |
| 5 | 24 | 7 | SNP |
| | 12 | 6 | Gene |
| | 14 | 4 | Feature |

**Table 3.** Comparison of different subsets of features in predicting control subjects or AD patients.

| | | Genetic | Clinical | Genetic + Clinical | Clinical - APOE - MMSE | Genetic + Clinical - APOE - MMSE |
|---|---|---|---|---|---|---|
| Training | Precision | 0.9633 | 1.0000 | 1.0000 | 0.9658 | 1.0000 |
| | Recall | 0.8537 | 1.0000 | 1.0000 | 0.9187 | 1.0000 |
| | F1 Score | 0.9052 | 1.0000 | 1.0000 | 0.9417 | 1.0000 |
| | Accuracy | 0.9396 | 1.0000 | 1.0000 | 0.9615 | 1.0000 |
| 2-fold CV | Precision | 0.7748 | 0.9280 | 0.9675 | 0.3774 | 0.7699 |
| | Recall | 0.6992 | 0.9431 | 0.9675 | 0.3252 | 0.7073 |
| | F1 Score | 0.7350 | 0.9355 | 0.9675 | 0.3493 | 0.7373 |
| | Accuracy | 0.8297 | 0.9560 | 0.9780 | 0.5907 | 0.8297 |
| LOO CV | Precision | 0.8100 | 0.9286 | 0.9600 | 0.3738 | 0.7596 |
| | Recall | 0.6585 | 0.9512 | 0.9756 | 0.3252 | 0.6423 |
| | F1 Score | 0.7265 | 0.9398 | 0.9677 | 0.3478 | 0.6960 |
| | Accuracy | 0.8324 | 0.9588 | 0.9780 | 0.5879 | 0.8104 |

'Genetic' is short for genetic features; 'Clinical' is short for clinical features. F1 Score = 2 × (Precision × Recall) / (Precision + Recall); 'Training' stands for the process of a single-loop CV; '2-fold CV' means that 2-fold CV was used in the external loop of double CV; 'LOO CV' means that LOO CV was used in the external loop of double CV.

**Table 4.** The statistical significance of genetic features selected by GenEpi in predicting patients with AD.

| Selected SNPs (RSID) | Weight | Odds Ratio | $\chi^2$-test P-value | Genotype Frequency | Gene |
|---|---|---|---|---|---|
| rs3130614_BB, rs41276317_AB | 3.16 | 19.23 | 1.42E-09 | 0.0742 | *MICB*TOB2* |
| rs12095538_BB, rs2774308_AB | 2.41 | 7.69 | 6.87E-07 | 0.0824 | *SYT6* |
| rs12926153_AB, rs12922908_AA | 1.18 | 4.83 | 6.89E-07 | 0.1511 | *CLEC16A* |
| rs9652600_AB, rs12922908_AA | 0.94 | 4.83 | 6.89E-07 | 0.1511 | *CLEC16A* |
| rs9344977_BB, rs56148686_AB | 1.94 | 4.32 | 1.14E-06 | 0.1813 | *BACH2* |
| rs429358_AA | -2.01 | 0.17 | 1.73E-06 | 0.5962 | *APOE* |
| rs56233035_AB, rs3678_AB | 2.26 | 10.16 | 1.91E-06 | 0.0604 | *CACNA1E* |
| rs11675339_AA, rs2710687_AA | 2.32 | 3.94 | 3.55E-06 | 0.1923 | *VSNL1* |
| rs12189429_BB, rs6881360_AA | 1.36 | 4.34 | 3.65E-06 | 0.467 | *ADAMTS12* |
| rs12187423_BB, rs6881360_AA | 0.58 | 4.34 | 3.65E-06 | 0.467 | *ADAMTS12* |
| rs10831829_BB, rs12366151_AA | 3.48 | 9.50 | 4.90E-06 | 0.0577 | *PARVA* |
| rs2052573_BB, rs34580133_AB | 1.80 | 4.08 | 5.00E-06 | 0.1648 | *LINC00299* |
| rs2421701_AB, rs200512701_AB | 1.82 | 4.12 | 5.29E-06 | 0.1593 | *TNKS2* |
| rs769449_AA | -1.19 | 0.16 | 8.42E-06 | 0.6648 | *APOE* |

The sign '*' between two gene symbols indicates cross-gene epistasis.

**Table 5.** Comparison of different subsets of features in predicting the progression of AD.

| | | Genetic | Clinical | Genetic + Clinical | Clinical - APOE | Genetic + Clinical - APOE |
|---|---|---|---|---|---|---|
| Training | Pearson | 0.4641 | 0.9582 | 0.9613 | 0.9533 | 0.9600 |
| | Spearman | 0.2939 | 0.9277 | 0.9375 | 0.9227 | 0.9385 |
| | AVG(P+S) | 0.3790 | 0.9430 | 0.9494 | 0.9380 | 0.9493 |
| 2-folds CV | Pearson | 0.4088 | 0.5014 | 0.5771 | 0.4896 | 0.5702 |
| | Spearman | 0.2286 | 0.4517 | 0.4915 | 0.4289 | 0.4776 |
| | AVG(P+S) | 0.3187 | 0.4765 | 0.5343 | 0.4593 | 0.5239 |
| LOO CV | Pearson | 0.4123 | 0.4922 | 0.5806 | 0.4741 | 0.5732 |
| | Spearman | -0.1032 | 0.4441 | 0.4960 | 0.4197 | 0.4854 |
| | AVG(P+S) | 0.1545 | 0.4682 | 0.5383 | 0.4469 | 0.5293 |

'Genetic' is short for genetic features; 'Clinical' is short for clinical features; 'Pearson' means Pearson's Correlation; 'Spearman' means Spearman's Correlation; 'AVG(P+S)' means the average of Pearson and Spearman correlations; 'Training' stands for the process of a single-loop CV; '2-fold CV' means that 2-fold CV was used in the external loop of double CV; 'LOO CV' means that LOO CV was used in the external loop of double CV.

**Table 6.** The statistical significance of genetic features selected by GenEpi in predicting the progression of AD.

| Selected SNPs (RSID) | Weight | T-test P-value | Genotype Frequency | Gene |
|---|---|---|---|---|
| rs2306894_BB, rs11653674_BB | -1.2045 | 5.53E-13 | 0.3025 | *CLEC1A*GPR142* |
| rs2306894_BB, rs4078431_BB | -0.8244 | 4.55E-13 | 0.0574 | *CLEC1A*PRKAG2-AS1* |
| rs7221462_BB, rs11721292_AA | 1.3215 | 3.09E-11 | 0.8905 | *IFT20*RPL32* |
| rs2242373_AA, rs4078431_BB | -1.2188 | 3.51E-13 | 0.0756 | *MFSD6L*PRKAG2-AS1* |

'*' sign between two gene symbols indicates cross-gene epistasis.

**Table 7.** The comparison of different algorithms.

| Algorithm | # Input SNP | Time Cost | Top 15 | Top 30 | Top 45 | Top 60 |
|---|---|---|---|---|---|---|
| Classification – Classifying AD patients | | | | | | |
| GenEpi | 4,916,249 | 9.95 | 0.76 | 0.72 | 0.71 | 0.68 |
| BOOST | 4,916,249 | 2157.6 | 0.31 | 0.24 | 0.30 | 0.37 |
| ReliefF | 33,868 | 0.11 | 0.52 | 0.48 | 0.45 | 0.46 |
| FastEpistasis | 12,809,667 | 836.8 | 0.62 | 0.61 | 0.60 | 0.59 |
| Regression – Predicting the progression of AD | | | | | | |
| GenEpi | 5,086,639 | 28.38 | 0.35 | 0.48 | 0.46 | 0.50 |
| BOOST | 5,086,639 | 327.12 | 0.08 | 0.08 | 0.05 | 0.04 |
| ReliefF | 69,842 | 1.05 | 0.16 | 0.22 | 0.23 | 0.26 |

Time is the time spent on identifying the epistasis, which was measured by single CPU time in days. The values in column top 15, top 30, top 45 and top 60 are the 2-fold CV scores. The 2-fold CV scores in classifying AD patients and predicting the progression of AD are the F1 scores and the average of Pearson and Spearman correlation, respectively.

# Declarations

**Ethics approval and consent to participate**

Not applicable.

**Consent for publication**

Not applicable.

**Availability of data and material**

Not applicable.

**Competing interests**

The authors declare that they have no competing interests.

**Funding**

This work has been supported by the Ministry of Science and Technology of Taiwan grant 105-2911-I-002-566, 105-2221-E-002-129-MY3 and 103-2627-M002-015.

**Authors' contributions**

Y.-C.C. initiated the study, designed the analysis procedures, performed the analysis and wrote the manuscript. J.-T.W. finished the literature survey of the epistasis that selected by GenEpi and wrote the discussion. C.-Y.C. is the main advisor of Y.-C.C., guided this research on right way and provided ideas to optimize the methods. Y.-C.C, M.-Y.H., Y.-A.T, C.-Y.C. and Y.-J.O. were team members of Alzheimer's disease Dream Challenge. C.-Y.C., Y.-J.O., P.-H.H. K.M.G. and S.W.Y. commented on the draft and revised the manuscript. All authors read and approved the final manuscript.

**Acknowledgements**

Data collection and sharing for this project was funded by the ADNI (National Institutes of Health Grant U01 AG024904). ADNI is funded by the National Institute on Aging, the National Institute of Biomedical Imaging and Bioengineering, and through generous contributions from the following: Abbott; Alzheimer's Association; Alzheimer's Drug Discovery Foundation; AmorfixLife Sciences Ltd.; AstraZeneca; Bayer HealthCare; BioClinica, Inc.; Biogen Idec Inc.;

Bristol-Myers Squibb Company; Eisai Inc.; Elan Pharmaceuticals Inc.; Eli Lilly and Company; F.Hoffmann-La Roche Ltd and its affiliated company Genentech, Inc.; GE Healthcare; Innogenetics, N.V.; Janssen Alzheimer Immunotherapy Research & Development, LLC.; Johnson & Johnson Pharmaceutical Research & Development LLC.; Medpace, Inc.; Merck & Co., Inc.; Meso Scale Diagnostics, LLC.; Novartis Pharmaceuticals Corporation; Pfizer Inc.; Servier; Synarc Inc. and Takeda Pharmaceutical Company. The Canadian Institutes of Health Research is providing funds to support ADNI clinical sites in Canada. Private sector contributions are facilitated by the Foundation for the National Institutes of Health (www.fnih.org). The grantee organization is the Northern California Institute for Research and Education and the study is coordinated by the Alzheimer's Disease Cooperative Study at the University of California, San Diego. ADNI data are disseminated by the Laboratory for Neuro Imaging at the University of California, Los Angeles. This research was also supported by NIH grants P30 AG010129, K01 AG030514 and the Dana Foundation.

608 ## Reference


609 1. Kingsmore SF, Lindquist IE, Mudge J, Gessler DD, Beavis WD: **Genome-wide**
610 **association studies: progress and potential for drug discovery and development**.
611 *Nature Reviews Drug Discovery* 2008, **7**(3):221-230.
612 2. Ozaki K, Ohnishi Y, Iida A, Sekine A, Yamada R, Tsunoda T, Sato H, Sato H, Hori M,
613 Nakamura Y *et al*: **Functional SNPs in the lymphotoxin-alpha gene that are**
614 **associated with susceptibility to myocardial infarction**. *Nat Genet* 2002, **32**(4):650-
615 654.
616 3. Klein RJ, Zeiss C, Chew EY, Tsai JY, Sackler RS, Haynes C, Henning AK, SanGiovanni
617 JP, Mane SM, Mayne ST *et al*: **Complement factor H polymorphism in age-related**
618 **macular degeneration**. *Science* 2005, **308**(5720):385-389.
619 4. Pinero J, Bravo A, Queralt-Rosinach N, Gutierrez-Sacristan A, Deu-Pons J, Centeno E,
620 Garcia-Garcia J, Sanz F, Furlong LI: **DisGeNET: a comprehensive platform**
621 **integrating information on human disease-associated genes and variants**. *Nucleic*
622 *Acids Res* 2017, **45**(D1):D833-D839.
623 5. McCarthy MI, Abecasis GR, Cardon LR, Goldstein DB, Little J, Ioannidis JP,
624 Hirschhorn JN: **Genome-wide association studies for complex traits: consensus,**
625 **uncertainty and challenges**. *Nat Rev Genet* 2008, **9**(5):356-369.
626 6. Eichler EE, Flint J, Gibson G, Kong A, Leal SM, Moore JH, Nadeau JH: **Missing**
627 **heritability and strategies for finding the underlying causes of complex disease**. *Nat*
628 *Rev Genet* 2010, **11**(6):446-450.
629 7. Manolio TA, Collins FS, Cox NJ, Goldstein DB, Hindorff LA, Hunter DJ, McCarthy
630 MI, Ramos EM, Cardon LR, Chakravarti A *et al*: **Finding the missing heritability of**
631 **complex diseases**. *Nature* 2009, **461**(7265):747-753.
632 8. Frazer KA, Murray SS, Schork NJ, Topol EJ: **Human genetic variation and its**
633 **contribution to complex traits**. *Nat Rev Genet* 2009, **10**(4):241-251.
634 9. Carlborg O, Haley CS: **Epistasis: too often neglected in complex trait studies?** *Nat*
635 *Rev Genet* 2004, **5**(8):618-625.
636 10. Cordell HJ: **Detecting gene-gene interactions that underlie human diseases**. *Nat Rev*
637 *Genet* 2009, **10**(6):392-404.
638 11. Easton DF, Pooley KA, Dunning AM, Pharoah PD, Thompson D, Ballinger DG,
639 Struewing JP, Morrison J, Field H, Luben R *et al*: **Genome-wide association study**
640 **identifies novel breast cancer susceptibility loci**. *Nature* 2007, **447**(7148):1087-1093.

12. Shriner D, Vaughan LK, Padilla MA, Tiwari HK: **Problems with genome-wide association studies**. *Science* 2007, **316**(5833):1840-1842.
13. Bodmer W, Bonilla C: **Common and rare variants in multifactorial susceptibility to common diseases**. *Nat Genet* 2008, **40**(6):695-701.
14. Hindorff LA, Sethupathy P, Junkins HA, Ramos EM, Mehta JP, Collins FS, Manolio TA: **Potential etiologic and functional implications of genome-wide association loci for human diseases and traits**. *Proc Natl Acad Sci U S A* 2009, **106**(23):9362-9367.
15. Moore JH, Asselbergs FW, Williams SM: **Bioinformatics challenges for genome-wide association studies**. *Bioinformatics* 2010, **26**(4):445-455.
16. Marchini J, Donnelly P, Cardon LR: **Genome-wide strategies for detecting multiple loci that influence complex diseases**. *Nat Genet* 2005, **37**(4):413-417.
17. Wei WH, Hemani G, Haley CS: **Detecting epistasis in human complex traits**. *Nat Rev Genet* 2014, **15**(11):722-733.
18. Schupbach T, Xenarios I, Bergmann S, Kapur K: **FastEpistasis: a high performance computing solution for quantitative trait epistasis**. *Bioinformatics* 2010, **26**(11):1468-1469.
19. Wan X, Yang C, Yang Q, Xue H, Fan X, Tang NL, Yu W: **BOOST: A fast approach to detecting gene-gene interactions in genome-wide case-control studies**. *Am J Hum Genet* 2010, **87**(3):325-340.
20. Purcell S, Neale B, Todd-Brown K, Thomas L, Ferreira MA, Bender D, Maller J, Sklar P, de Bakker PI, Daly MJ *et al*: **PLINK: a tool set for whole-genome association and population-based linkage analyses**. *Am J Hum Genet* 2007, **81**(3):559-575.
21. Chang CC, Chow CC, Tellier LC, Vattikuti S, Purcell SM, Lee JJ: **Second-generation PLINK: rising to the challenge of larger and richer datasets**. *Gigascience* 2015, **4**:7.
22. Moore JH, Williams SM: **New strategies for identifying gene-gene interactions in hypertension**. *Ann Med* 2002, **34**(2):88-95.
23. Yang P, Ho JW, Yang YH, Zhou BB: **Gene-gene interaction filtering with ensemble of filters**. *BMC Bioinformatics* 2011, **12 Suppl 1**:S10.
24. Bureau A, Dupuis J, Falls K, Lunetta KL, Hayward B, Keith TP, Van Eerdewegh P: **Identifying SNPs predictive of phenotype using random forests**. *Genet Epidemiol* 2005, **28**(2):171-182.
25. Schwarz DF, Konig IR, Ziegler A: **On safari to Random Jungle: a fast implementation of Random Forests for high-dimensional data**. *Bioinformatics* 2010, **26**(14):1752-1758.

26. Wan X, Yang C, Yang Q, Xue H, Tang NL, Yu W: **MegaSNPHunter: a learning approach to detect disease predisposition SNPs and high level interactions in genome wide association study**. *BMC Bioinformatics* 2009, **10**:13.
27. Murk W, DeWan AT: **Exhaustive Genome-Wide Search for SNP-SNP Interactions Across 10 Human Diseases**. *G3 (Bethesda)* 2016, **6**(7):2043-2050.
28. Allen GI, Amoroso N, Anghel C, Balagurusamy V, Bare CJ, Beaton D, Bellotti R, Bennett DA, Boehme KL, Boutros PC *et al*: **Crowdsourced estimation of cognitive decline and resilience in Alzheimer's disease**. *Alzheimers Dement* 2016, **12**(6):645-653.
29. Ma L, Clark AG, Keinan A: **Gene-based testing of interactions in association studies of quantitative traits**. *PLoS Genet* 2013, **9**(2):e1003321.
30. Oh S, Lee J, Kwon MS, Weir B, Ha K, Park T: **A novel method to identify high order gene-gene interactions in genome-wide association studies: gene-based MDR**. *BMC Bioinformatics* 2012, **13 Suppl 9**:S5.
31. Li S, Cui Y: **Gene-centric gene–gene interaction: A model-based kernel machine method**. *The Annals of Applied Statistics* 2012, **6**(3):1134-1161.
32. Wu X, Dong H, Luo L, Zhu Y, Peng G, Reveille JD, Xiong M: **A novel statistic for genome-wide interaction analysis**. *PLoS Genet* 2010, **6**(9):e1001131.
33. Kent WJ, Sugnet CW, Furey TS, Roskin KM, Pringle TH, Zahler AM, Haussler D: **The human genome browser at UCSC**. *Genome Res* 2002, **12**(6):996-1006.
34. Rosenbloom KR, Armstrong J, Barber GP, Casper J, Clawson H, Diekhans M, Dreszer TR, Fujita PA, Guruvadoo L, Haeussler M *et al*: **The UCSC Genome Browser database: 2015 update**. *Nucleic Acids Res* 2015, **43**(Database issue):D670-681.
35. Lewontin RC: **The Interaction of Selection and Linkage. I. General Considerations; Heterotic Models**. *Genetics* 1964, **49**(1):49-67.
36. Meinshausen N, Bühlmann P: **Stability selection**. *Journal of the Royal Statistical Society: Series B (Statistical Methodology)* 2010, **72**(4):417-473.
37. Urbanowicz RJ, Meeker M, LaCava W, Olson RS, Moore JH: **Relief-Based Feature Selection: Introduction and Review**. *arXiv preprint arXiv:171108421* 2017.
38. Urbanowicz RJ, Kiralis J, Sinnott-Armstrong NA, Heberling T, Fisher JM, Moore JH: **GAMETES: a fast, direct algorithm for generating pure, strict, epistatic models with random architectures**. *BioData Min* 2012, **5**(1):16.
39. Consortium GT: **The Genotype-Tissue Expression (GTEx) project**. *Nat Genet* 2013, **45**(6):580-585.

40. Liddelow SA, Guttenplan KA, Clarke LE, Bennett FC, Bohlen CJ, Schirmer L, Bennett ML, Munch AE, Chung WS, Peterson TC *et al*: **Neurotoxic reactive astrocytes are induced by activated microglia**. *Nature* 2017, **541**(7638):481-487.
41. von Bernhardi R, Ramirez G: **Microglia-astrocyte interaction in Alzheimer's disease: friends or foes for the nervous system?** *Biol Res* 2001, **34**(2):123-128.
42. Raj D, Yin Z, Breur M, Doorduin J, Holtman IR, Olah M, Mantingh-Otter IJ, Van Dam D, De Deyn PP, den Dunnen W *et al*: **Increased White Matter Inflammation in Aging- and Alzheimer's Disease Brain**. *Front Mol Neurosci* 2017, **10**:206.
43. Ward LD, Kellis M: **HaploReg: a resource for exploring chromatin states, conservation, and regulatory motif alterations within sets of genetically linked variants**. *Nucleic Acids Res* 2012, **40**(Database issue):D930-934.
44. Li P, Lahvic JL, Binder V, Pugach EK, Riley EB, Tamplin OJ, Panigrahy D, Bowman TV, Barrett FG, Heffner GC *et al*: **Epoxyeicosatrienoic acids enhance embryonic haematopoiesis and adult marrow engraftment**. *Nature* 2015, **523**(7561):468-471.
45. Kim E, Lee SH, Lee KS, Cheong HK, Namkoong K, Hong CH, Oh BH: **AMPK gamma2 subunit gene PRKAG2 polymorphism associated with cognitive impairment as well as diabetes in old age**. *Psychoneuroendocrinology* 2012, **37**(3):358-365.
46. Peixoto CA, Oliveira WH, Araujo S, Nunes AKS: **AMPK activation: Role in the signaling pathways of neuroinflammation and neurodegeneration**. *Exp Neurol* 2017, **298**(Pt A):31-41.
47. Whitfield JF, Chiarini A, Dal Pra I, Armato U, Chakravarthy B: **The Possible Roles of the Dentate Granule Cell's Leptin and Other Ciliary Receptors in Alzheimer's Neuropathology**. *Cells* 2015, **4**(3):253-274.
48. Vivier E, Tomasello E, Paul P: **Lymphocyte activation via NKG2D: towards a new paradigm in immune recognition?** *Curr Opin Immunol* 2002, **14**(3):306-311.
49. Collins RW: **Human MHC class I chain related (MIC) genes: their biological function and relevance to disease and transplantation**. *Eur J Immunogenet* 2004, **31**(3):105-114.
50. Quiroga I, Lehmann DJ, Barnardo MC, Fuggle S, Cortina-Borja M, Warden DR, Smith AD: **Association study of MICA and MICB in Alzheimer's disease**. *Tissue Antigens* 2009, **74**(3):241-243.
51. Mirza Z, Rajeh N: **Identification Of Electrophysiological Changes In Alzheimer's Disease: A Microarray Based Transcriptomics And Molecular Pathway Analysis**

**Study**. *CNS Neurol Disord Drug Targets* 2017.

52. Saura CA, Parra-Damas A, Enriquez-Barreto L: **Gene expression parallels synaptic excitability and plasticity changes in Alzheimer's disease**. *Front Cell Neurosci* 2015, **9**:318.

53. Daschil N, Obermair GJ, Flucher BE, Stefanova N, Hutter-Paier B, Windisch M, Humpel C, Marksteiner J: **CaV1.2 calcium channel expression in reactive astrocytes is associated with the formation of amyloid-beta plaques in an Alzheimer's disease mouse model**. *J Alzheimers Dis* 2013, **37**(2):439-451.

54. Porcellini E, Carbone I, Ianni M, Licastro F: **Alzheimer's disease gene signature says: beware of brain viral infections**. *Immun Ageing* 2010, **7**:16.

55. Talkowski ME, Maussion G, Crapper L, Rosenfeld JA, Blumenthal I, Hanscom C, Chiang C, Lindgren A, Pereira S, Ruderfer D *et al*: **Disruption of a large intergenic noncoding RNA in subjects with neurodevelopmental disabilities**. *Am J Hum Genet* 2012, **91**(6):1128-1134.

56. Uhrig M, Ittrich C, Wiedmann V, Knyazev Y, Weninger A, Riemenschneider M, Hartmann T: **New Alzheimer amyloid beta responsive genes identified in human neuroblastoma cells by hierarchical clustering**. *PLoS One* 2009, **4**(8):e6779.

57. Wang W, Mandel J, Bouaziz J, Commenges D, Nabirotchkine S, Chumakov I, Cohen D, Guedj M, Alzheimer's Disease Neuroimaging I: **A Multi-Marker Genetic Association Test Based on the Rasch Model Applied to Alzheimer's Disease**. *PLoS One* 2015, **10**(9):e0138223.

58. Babic Leko M, Borovecki F, Dejanovic N, Hof PR, Simic G: **Predictive Value of Cerebrospinal Fluid Visinin-Like Protein-1 Levels for Alzheimer's Disease Early Detection and Differential Diagnosis in Patients with Mild Cognitive Impairment**. *J Alzheimers Dis* 2016, **50**(3):765-778.

59. Kirkwood CM, MacDonald ML, Schempf TA, Vatsavayi AV, Ikonomovic MD, Koppel JL, Ding Y, Sun M, Kofler JK, Lopez OL *et al*: **Altered Levels of Visinin-Like Protein 1 Correspond to Regional Neuronal Loss in Alzheimer Disease and Frontotemporal Lobar Degeneration**. *J Neuropathol Exp Neurol* 2016, **75**(2):175-182.

60. Luo X, Hou L, Shi H, Zhong X, Zhang Y, Zheng D, Tan Y, Hu G, Mu N, Chan J *et al*: **CSF levels of the neuronal injury biomarker visinin-like protein-1 in Alzheimer's disease and dementia with Lewy bodies**. *J Neurochem* 2013, **127**(5):681-690.

61. Pietrzak M, Rempala G, Nelson PT, Zheng JJ, Hetman M: **Epigenetic silencing of nucleolar rRNA genes in Alzheimer's disease**. *PLoS One* 2011, **6**(7):e22585.

62. Rouillard AD, Gundersen GW, Fernandez NF, Wang Z, Monteiro CD, McDermott MG, Ma'ayan A: **The harmonizome: a collection of processed datasets gathered to serve and mine knowledge about genes and proteins**. *Database (Oxford)* 2016, **2016**.

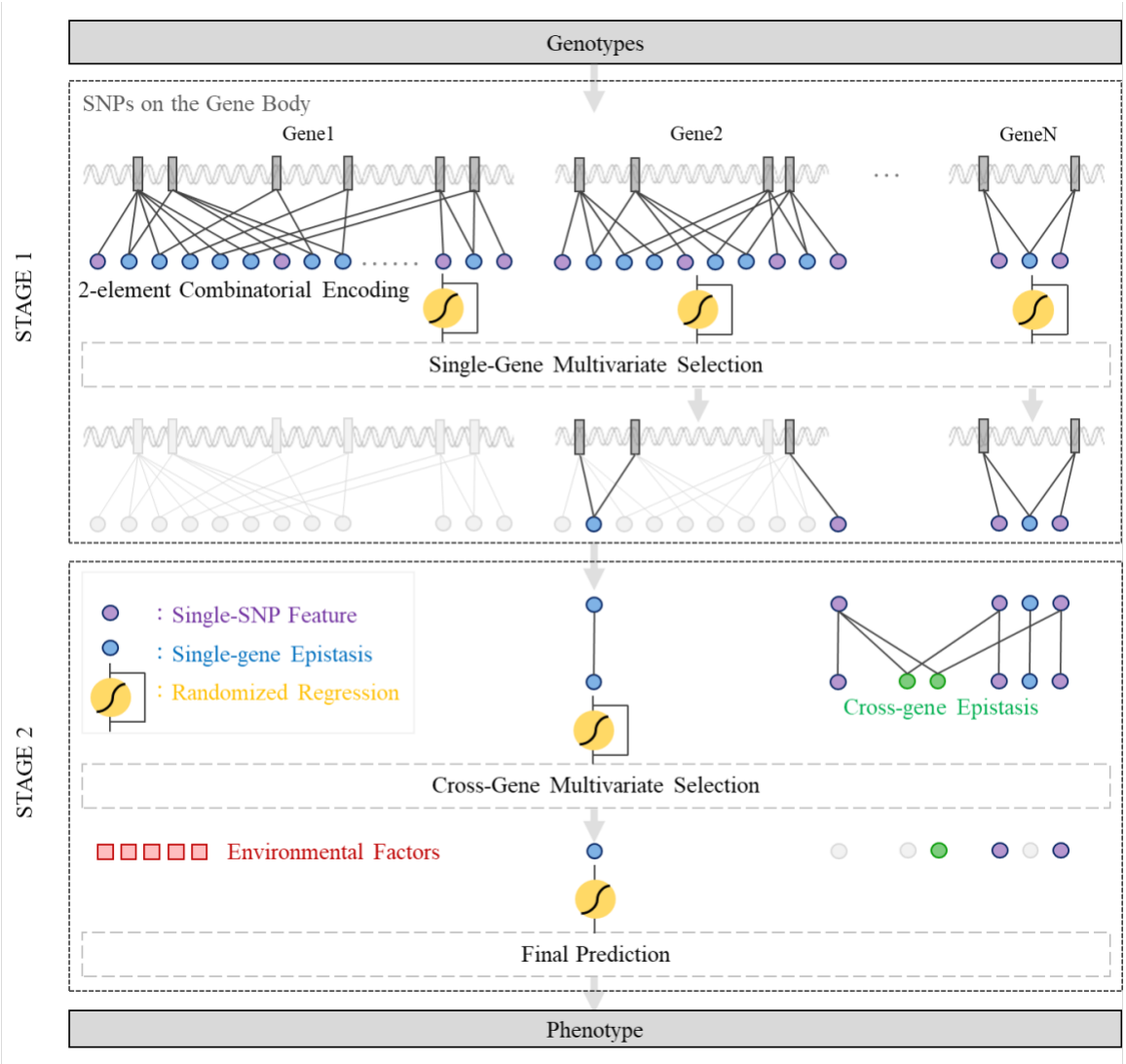


**Fig. 1.** The architecture of GenEpi.

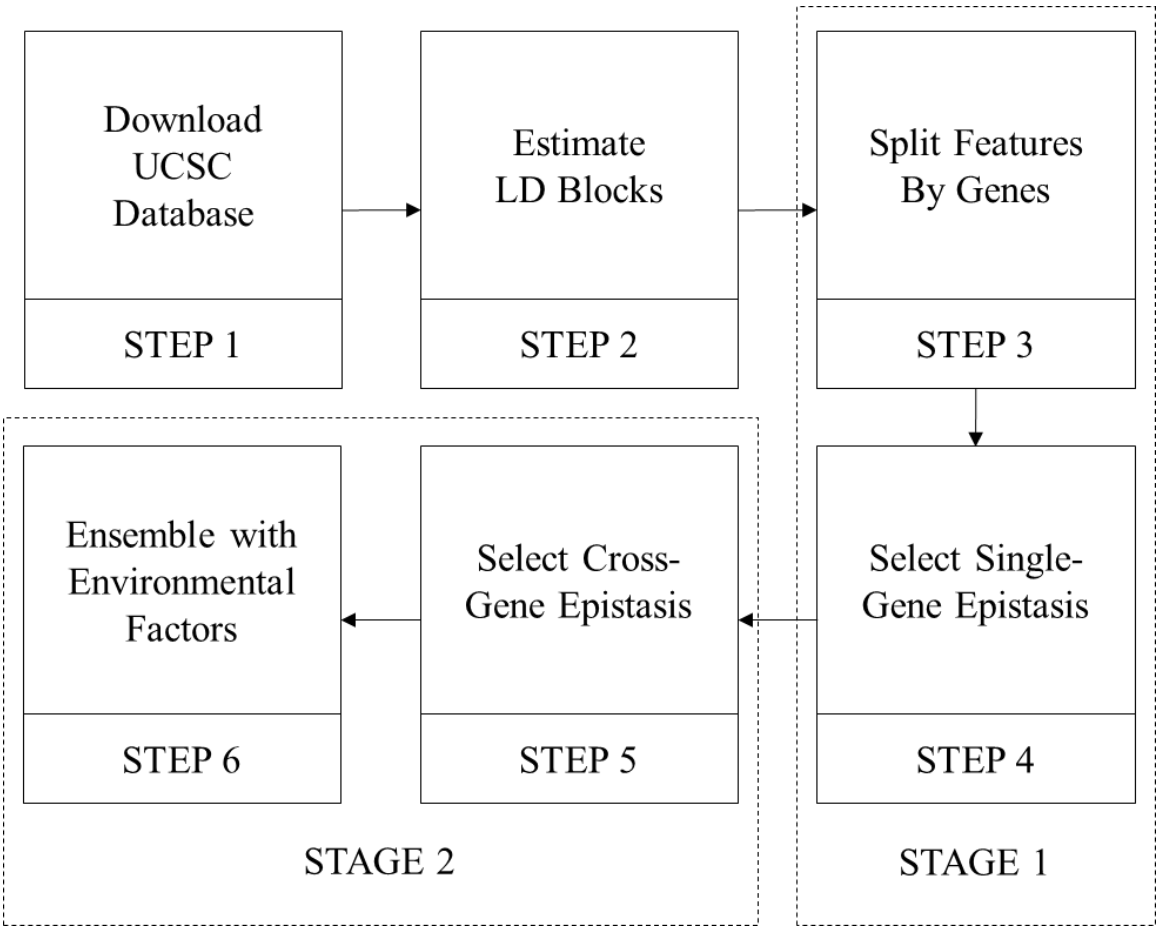


**Fig. 2.** The modules and data flow in the proposed GenEpi Python package. The first and second modules (STEP 1 and STEP 2) are the two pre-processing steps for downloading the UCSC database and reducing the dimension using LD. The third and fourth modules (STEP 3 and STEP 4) correspond to the STAGE 1 of GenEpi, and the final two modules (STEP 5 and STEP 6) correspond to the STAGE 2 of GenEpi.

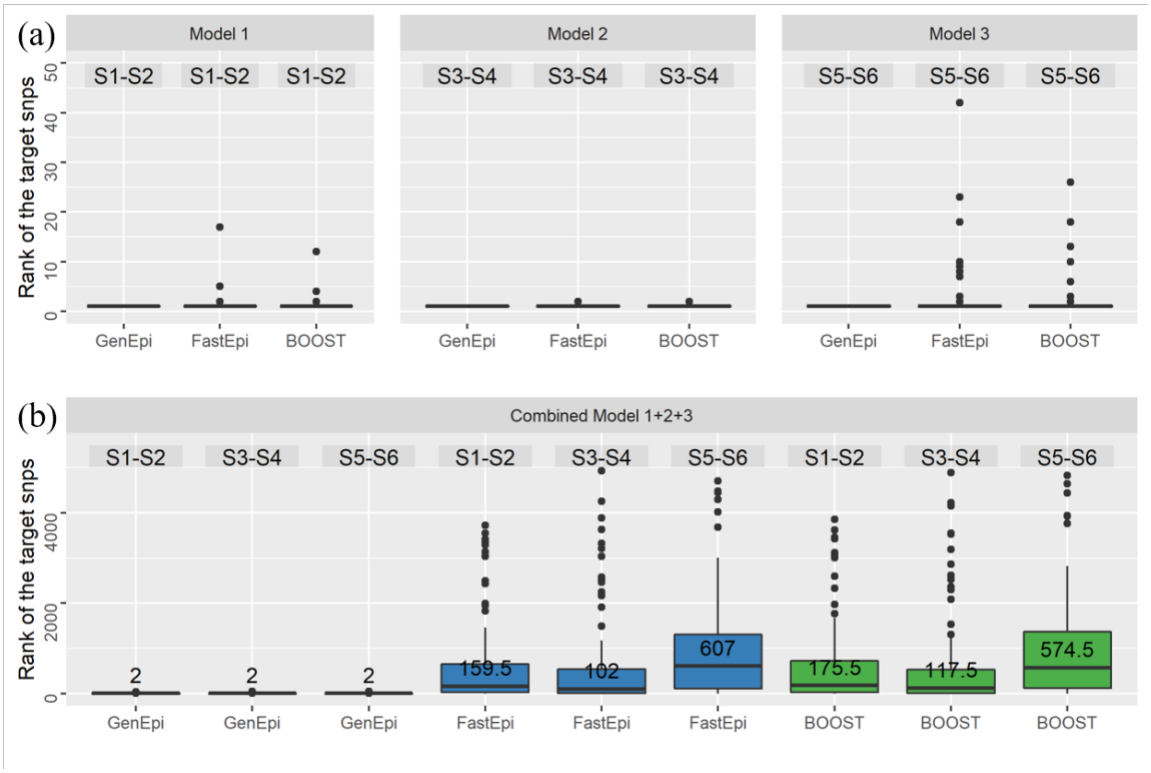


**Fig. 3.** The boxplot for the rank of the target epistasis in different algorithms. (a) The results of three basic-model datasets with one epistasis consisting of a SNP pair. (b) The result of the complex-model dataset, which contained three epistasis. The 'S1-S2' means the epistasis between SNP 1 and SNP 2 and so on. The values on the boxplot are the medians of the rank of the target epistasis among the 100 runs of simulation.

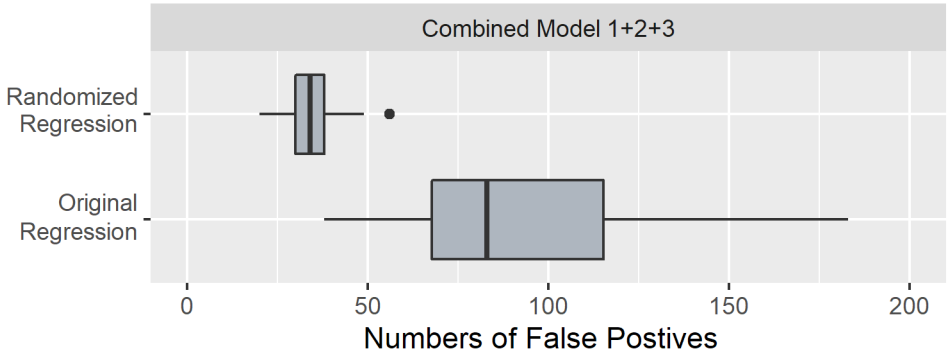


**Fig. 4.** The numbers of false positives in randomized and original regression.

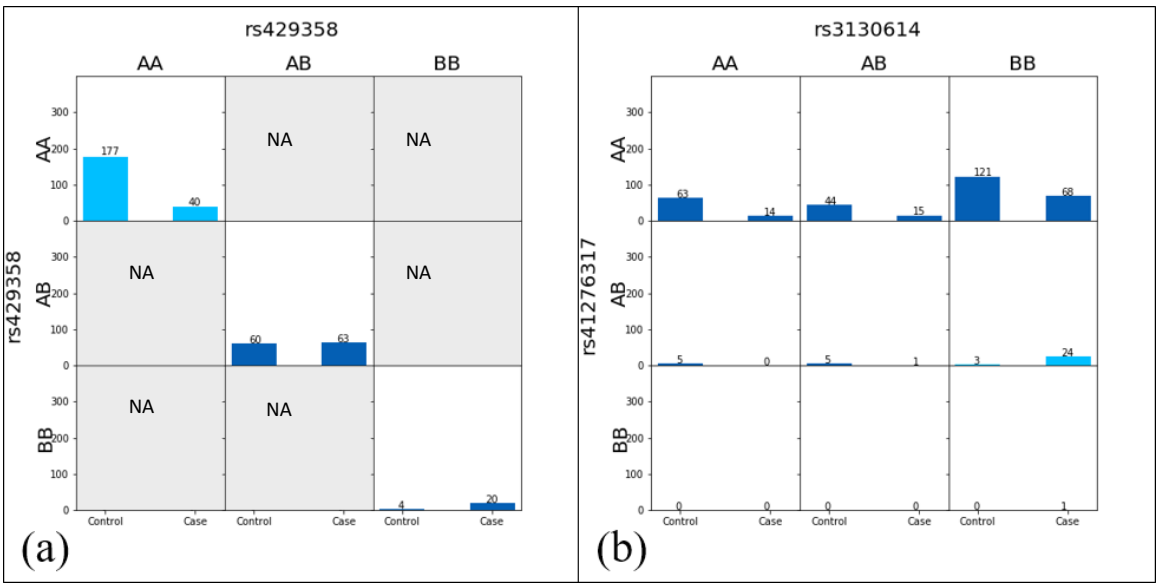


**Fig. 5.** (a) The bar plot for the population of three allele types in rs429358. (b) The bar plot for combinations of SNPs from the cross-gene epistasis feature selected by GenEpi in predicting control subjects or AD patients. The color 'light blue' is used to highlight the features selected by GenEpi.

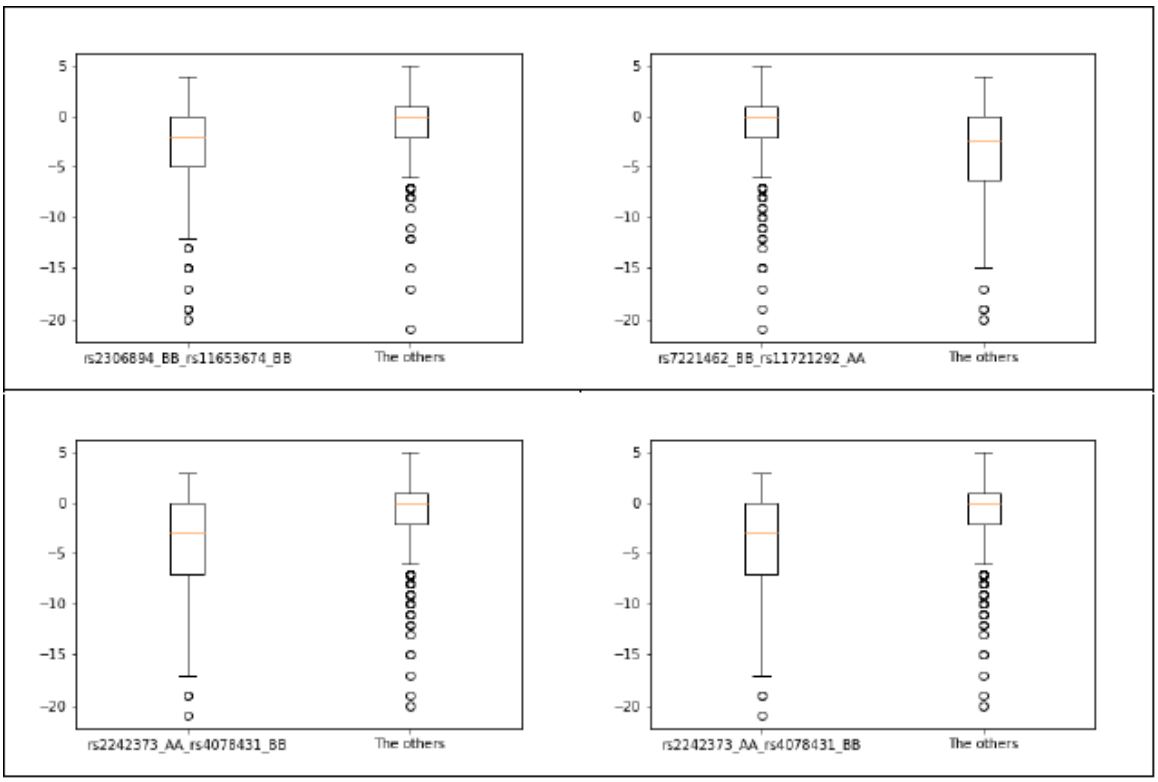


**Fig. 6.** The box plots for combinations of SNPs from the genetic features selected by GenEpi in predicting the progression of AD. The y-axes of the plot are MMSE difference between '24-month follow-up MMSE' and 'MMSE at baseline'.

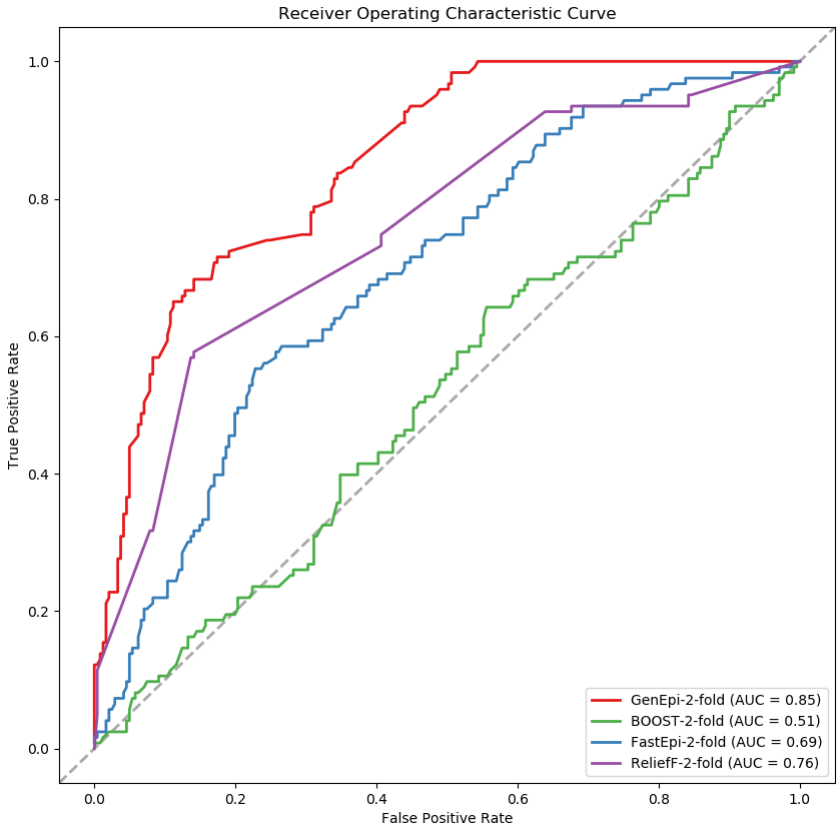


**Fig. 7.** The ROC curves of different algorithms.

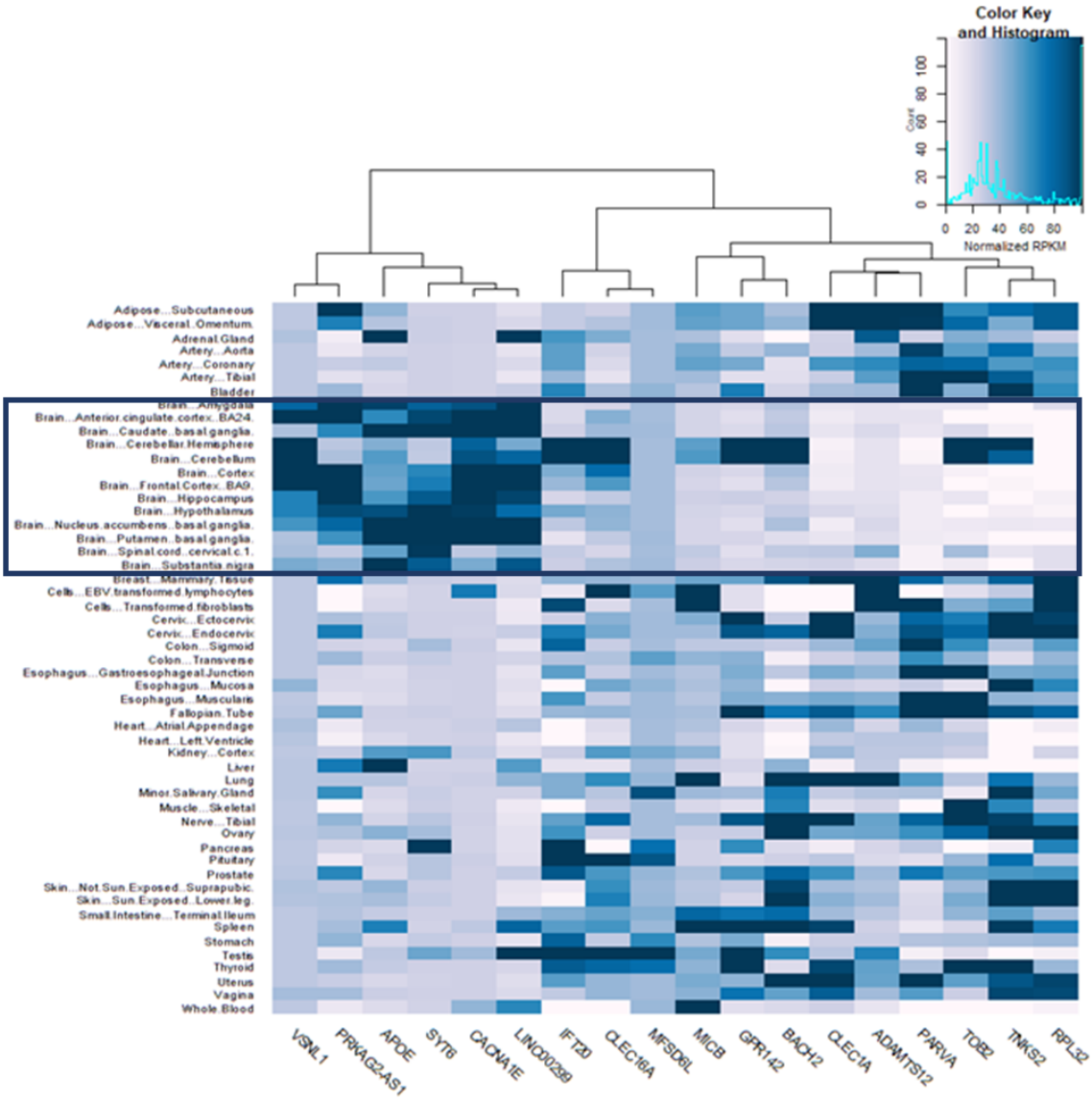


**Fig. 8.** The heatmap of gene expression in different tissues for the 18 genes selected by GenEpi. The blue box highlights the sub-regions of brain.